

COMPLETE COMPUTATIONAL MODEL OF A HALL THRUSTER FROM THE ACCELERATION CHANNEL THROUGH THE PLUME

Salma Qarnain* and Daniel E. Hastings†
Department of Aeronautics and Astronautics
Massachusetts Institute of Technology
Cambridge, MA

Abstract

Two- and three-dimensional computational models describing both the internal¹ and external² physics of Hall thrusters have been developed at the Massachusetts Institute of Technology. Integration of these models would result in a single, stand-alone application characterizing thruster physics from the thruster interior through the plume region. The application would enhance the spacecraft design process by providing engineers with the ability to predict thruster performance and damage to the craft from plume-spacecraft interactions. This paper represents the first attempt at consolidation of the internal and external computational models, exploring the issues critical to integration.

The key issue in integration is the compatibility between the source model produced by the acceleration channel code and the source model used by the three-dimensional plume code. Sensitivity analysis has been performed to determine the extent to which the source model affects the plume and the surrounding spacecraft surface. Results on a realistic spacecraft geometry suggest that differences between the original source model and the model generated by the acceleration channel code significantly affect satellite surface erosion rates. Enhancements have also been made to the source and sputtering models in the plume code. Results utilizing the improved source model have been validated against experimental data and suggest that the source axial ion temperature assumed in previous work² was over predicted. In addition, the sputtering model now includes the effect of the sputtering yield dependence upon particle angle of incidence.

Future work includes a graphical user interface on X-windows platforms, automatic source model generation, and code stream-lining and optimization.

Nomenclature

T_e = Electron Temperature
 r = Radial Distance from Anode Center
 z = Axial Distance from Anode Exit
 ϕ = Electrical Potential
 S = Sputtering Coefficient
 E = Total Ion Energy
 θ = Angle of Incidence

Introduction

Electric propulsion is at the forefront of space propulsion systems designed to reduce mission cost by reducing fuel mass required by the system. One promising electrostatic thruster is the Stationary Plasma Thruster (SPT), or the Hall Thruster. This device has a near optimum specific impulse for north-south stationkeeping and is currently being actively marketed for use on Western satellites. Consequently, satellite designers are demanding detailed understanding of the thruster's operation and interaction with the spacecraft. Engineers, however, lack reliable experimental data on the operation of this thruster and on the thruster plume-spacecraft interactions. This makes computational modeling a necessity. As a result, two- and three-dimensional models have been developed to study the physics of Hall thrusters and to simulate the interaction phenomenon between the spacecraft and the thruster plume.

A two-dimensional model of the Hall thruster acceleration chamber was developed by Fife in 1995.¹ The model is used to generate predictive information concerning the thrust, torque, power, and efficiency of the thruster, as well as providing thruster wall erosion rates. Compared with experimental data, the model is accurate to

*Research Assistant and S.M. Candidate

†Professor of Aeronautics and Astronautics

within 7% in thrust, torque, power, and efficiency predictions.

A substantial amount of experimental work has been conducted on plume contamination issues. Ion fluxes and distributions have been determined and plume-induced sputtering and contamination have been measured in several ground experiments. Until 1995, however, relatively little effort had been made to model processes occurring in the SPT's plume region. The plume model, developed by Oh² and validated against experimental data, fully characterizes the processes inside the plume region.

This paper presents the key integration issues facing the generation of a complete computational model of a Hall thruster. The model would combine the hybrid Particle-in-Cell (PIC) method for the interior of the thruster with the combination Particle-in-Cell (PIC) and Direct Simulation Monte Carlo (DSMC) method to simulate collisions in the plume and track the flow of ions and neutrals across the domain. The hybrid-PIC and basic PIC-DSMC algorithms have been described in previous work.^{1,2,3} Improvements have been made to the plume model, including the addition of the surface sputtering yield dependence on angle of incidence and the development of an improved source model. The resulting integrated model would run on a UNIX workstation and would be useful to designers interested in evaluating the impact of an SPT on realistic satellite configurations.

Section 2 summarizes the hybrid-PIC model of the thruster acceleration channel and describes the aspects of the hybrid-PIC and the PIC-DSMC algorithms specific to integration. This section also details the enhancements to the plume model. Section 3 presents the results of the sensitivity analysis of the plume model to source inputs as well as improved source and sputtering model results, and future work is outlined. Finally, Section 4 presents the conclusions.

Theory and Computational Method

Hybrid PIC Model

A hybrid Particle-in-Cell (PIC) method was used to simulate the physics of plasma within the acceleration channel of a Hall thruster. The model has predicted thrust, torque, power, and thruster efficiency to within 7% of experimental values. This level of accuracy makes the hybrid-PIC code appropriate as a design tool in

understanding thruster operating conditions using a variety of thruster geometries.

The hybrid-PIC model has been described in detail in previous work.¹ This section briefly summarizes the basic algorithm and describes aspects of the model specific to integration, such as ionization behavior and low-frequency discharge oscillations.

A variety of thruster geometries can be utilized as input to the hybrid-PIC model. The SPT-100 was selected as the baseline configuration. Table 1 displays the operating conditions chosen for source model comparison tests described in the following section.

Inner Anode Diameter	68.8 mm
Outer Anode Diameter	100 mm
Propellant	Xe
Propellant Flow Rate	5.0 mg./sec.
Potential (ϕ)	300 V
Electron Temperature (T_e)	3 eV
Fraction of Ions which are Double Ions	0%

Table 1: SPT-100 Characteristics in Hybrid-PIC model

Electrons are modeled as Maxwellian fluid, with particles having a Maxwellian velocity distribution. Heavy species are treated as discrete particles and modeled using a modified-PIC method. The combination of treating electrons as a fluid and heavy species using a PIC method gives rise to the term "hybrid-PIC" scheme.

Collisions are limited to electron-neutral ionization. Ion-neutral momentum exchange is neglected, since the mean free path is large in most regions for both ions and neutral particles. During ionization, only single ions are assumed to be formed. The formation of double ions is not treated in the model.⁴

The ionization method determines the energy with which particles exit as well as the beam divergence angle. Thus, ionization mechanics plays an important role in the integration of the hybrid-PIC model with the plume model described in the following section. The ion distribution at the thruster exit plane generated by the hybrid-PIC model would serve as input to the plume model. Hence, the distribution must be correct in both composition and in beam divergence angle to yield accurate results from the plume code.

Another issue concerning the integration of the hybrid-PIC model with the plume model is low-frequency discharge oscillations. During operation, ionization current, anode current, and beam current, experience oscillations on the order of 30kHz. Thus, time-averaging must be employed to generate a quasi-steady-state exit plane distribution in ion current density and beam divergence. In addition, the hybrid-PIC code under predicts the oscillatory behavior due to an under prediction in electron temperature.⁵

PIC-DSMC Model

The model utilizes a computational scheme which combines Particle-in-Cell (PIC) and Direct Simulation Monte Carlo (DSMC) methods to address the physics of expanding plasma plumes and the plume's interactions with the spacecraft. Large-scale plume structures with realistic thruster geometries, as well as erosion of surface materials such as silver, quartz, and silicon, can be accurately simulated. The result is the first use of such a PIC-DSMC scheme in an application and the first comprehensive numerical model of a Hall Thruster plume.

The PIC-DSMC model used in this paper has been described in detail in previous work.³ This section describes aspects of the model specific to integration. In particular, enhancements to the three-dimensional plume source model and sputtering model are discussed.

Source Model

The plume code's source model is of key importance in the integration of the thruster acceleration chamber and plume models, since the source is the sole interface between the hybrid-PIC and the PIC-DSMC codes. Thus, output from the hybrid-PIC model must be compatible with the plume code for a complete simulation to operate accurately.

The source model for the plume code, however, is based upon only one set of empirical data for ion current density and beam divergence angle near the thruster exit plane.⁶ Thus, the code has not been extensively tested with a variety of source model inputs. The data for the existing source model is also suspect: no error bars are present in the data, and the asymmetric shape of the ion current density distribution suggests that the thruster has seen some damage or wear.

A second source model was created from the output of the hybrid-PIC code to quantify the sensitivity of the plume code to variations in source input and to gauge the compatibility of the interior and exterior thruster models. The source model is comprised of a probability distribution function and a beam divergence angle function. The distribution function gives the probability an ion will cross the exit plane at a radial distance less than a given location, r , while the beam divergence function provides the angle measured from the thruster centerline at which an ion crosses the thruster exit. A battery of tests were run using the different combinations of distribution and beam divergence functions in the plume model to measure the impact of the source on the model results.

A secondary issue regarding the source model concerns the axial ion temperature at the thruster exit plane. Although the assumptions upon which the original plume code results were based allow the accurate simulation of macroscopic properties of the plume, these same assumptions fail at the microscopic level. Inconsistencies appear between the energy data produced by the code and experimental data. Figure 1 and 2 show the experimental Retarding Analyzer Potential (RPA) data and simulated data. RPA data taken in an arc 60 cm away from the thruster exit indicate that there is a similar energy distribution of particles at a variety of angles away from the thruster centerline. The model, however, predicts a distribution in which the energy curve's peak shifts towards decreasing energy as the angle increases away from the centerline. This shift in the peak of the ion energy can be readily seen in Figure 2. Corrections to the axial ion temperature assumed in the source model have explained this behavior and have allowed the matching of the simulation with experiment at the microscopic level.

Sputtering Model

One issue of particular interest to satellite designers is the interaction of the plume with surfaces of a spacecraft. In order to study surface interaction issues, a surface sputtering model has been developed and incorporated into the PIC-DSMC model. The model, described below, is based upon a relatively simple model used for axisymmetric geometries.⁸

The SPT plume's primary impact on surfaces is to cause sputter-induced erosion damage. Plume-induced

deposition, however, is ignored in the model. Deposition can be safely ignored when modeling thrusters with ceramic anodes. In these cases, the eroded material is likely to be benign. In three-dimensional geometries, any particle crossing an object boundary is removed or reflected as appropriate for that species. Ions are neutralized and removed from the simulation, while neutrals are reflected back into the domain in a manner consistent with an ideal specular surface.

Sputtering rates are calculated by tabulating the material removed by each particle striking the simulated surfaces of the spacecraft. The amount of material lost is determined by multiplying an energy-dependent sputtering coefficient by the macroparticle weighting factor. A particle's impact energy is given by the sum of its kinetic energy and the energy gained or lost in the sheath. Neutrals are assumed to undergo no acceleration in the sheath region.

The erosion rate has been calculated for silver, which is commonly used for solar cell interconnectors. The following linear fit was used for its sputtering coefficient:⁷

$$S = 7.334 \times 10^{-3} E - 0.29511.$$

An enhancement made to the sputtering model is the inclusion of angular dependence of the sputtering yield. Previously, all particles were assumed to strike normal to the surface. However, it has been observed that the atoms striking at non-normal angles may have higher sputtering coefficients than those striking normal to the surface.¹¹ As a result, the surface model tended to under predict the erosion rate.

Although the angular dependence for xenon sputtering silver is unknown, a worst-case can be constructed from existing sputtering data. As Figure 3 shows, the sputtering yield for xenon into molybdenum increases over the normal yield by as much as a factor of six at angles between 70° and 80° from the normal.⁸ This can be taken as a worst case, since data is available for a few sputtering cases and only for high-energy sputtering. The energy dependence in the correction to the sputtering term is yet unknown.

Sensitivity Analysis

The sensitivity of the 3D plume model to the source is measured as the response of the erosion rate to various source models. Since designers are concerned with the plume-induced erosion effects on spacecraft surfaces, the

erosion rate becomes a logical choice for the systematic quantification of sensitivity to the source model. Different sources vary in the angle at which the ions exit the thruster as well as in the ion distribution at the exit plane. Consequently, that variation yields variability in erosion rates.

The major motivation for developing a three-dimensional plume model is to simulate realistic spacecraft geometries. The baseline satellite configuration chosen for the sensitivity analysis is shown in Figure 4. A simulated bus, yoke, and solar array are shown on a 3.2 m x 4.4 m x 3.2 m computational domain, and an embedded grid is visible along the edge of the main bus. This grid is collocated with the thruster and is used to better resolve the core of the plume. The section of bus shown has dimensions of 1.1 m x 1 m x 2.6 m and represents a quarter of the spacecraft's main bus. A 1.9 meter yoke connects the bus to the end of a solar array. The array is 1.5 meters wide and continues off the top of the domain. Only the bottom 2.7 meters of the array are included in the simulation, since it is this area which should experience the most plume-induced degradation.

Results and Discussion

Source Model

Full 3D plume model validation was achieved by matching the plume properties with experimental data at the microscopic level. The peak shift seen in Figure 2 suggested that ions exiting the thruster at angles further from the thruster centerline were of lower energies than those along the centerline. However, experimental data contradicts this prediction. In Figure 1, the actual energy peak does not shift as ion energy is sampled at angles further from the thruster centerline.

The physical explanation for the shift is related to the ion temperature used in the source model. Originally, the ions were assumed to have thermal energies of 34 eV, allowing the thermal velocity of the ions to be greater than in the empirical data by an order of magnitude. The added energy pushes most of the ions around the centerline, while the lower energy ions are turned outward by the electric field. Thus, fewer ions with lower energies will be found at angles away from the centerline.

If the source ion thermal energy were decreased, however, the ions would all be affected in the same

manner. Thus, although fewer ions would be seen at larger angles, the ion energy distribution would be similar at all angles, since all ions would have the same probability of reaching a given sampling location.

The axial ion temperature at the source was varied to test this theory of thermal shifting. Figures 2 and 5 give the energy distribution taken in an arc 60 cm from the thruster exit under differing axial ion temperatures. The effect of increasing the axial ion temperature is clear: increasing ion temperature at the source increases ion thermal velocity, which then acts to keep the particle along the centerline and does not allow for a more variable motion experienced by a particle with a low axial thermal velocity. The peak in the distribution of energies would then shift with higher energy particles, due to the inflated ion temperature, maintaining a path along the centerline. In order to correct the model and to match experimental data, an ion temperature on the order of a few eV's must be selected. This issue is further discussed, and a derivation is presented in previous work.²

As mentioned previously, two source models were constructed for the 3D plume model for integration testing. The first was based upon experimental data, while the second was taken from the output of the hybrid-PIC code. The plume model was run using the two sources, and RPA energy data was sampled in an arc 60 cm away from the thruster exit.

Figure 5 displays the RPA distribution at various angles away from the thruster centerline using the original experimental data. An axial ion temperature of 3.4 eV was used in the simulation. The RPA distribution for the model constructed from the hybrid-PIC code is given in Figure 6. The energy distributions are similar to each other in shape. As the graphs show, the hybrid-PIC code model populates angles away from the thruster centerline with ions as compared to the original data. This difference is quantified in the following section by the sensitivity analysis for both source models.

An important item to note is the nature of the hybrid-PIC source model. The ion current density generated by the model of the exit plane is nearly flat, suggesting that there are no ion losses to the walls. Losses would result in a parabolic curve, similar to Couette flow in a pipe. Ionizing collisions in the hybrid-PIC model are determined solely by electron-neutral interaction, and ionization occurs along constant- T_e magnetic field lines. Thus, the

ions are formed with similar energies via electron-neutral collisions at various distances, r , along the thruster with no losses to the wall.

In summary, previous assumptions made concerning the axial ion temperature proved to be invalid. Temperatures of an order of a magnitude lower must be used to match experimental data at the energy level. Also, differences in the distribution of particles at the exit plane yield differing energy distribution data in an arc 60 cm from the thruster exit. Although this is not a surprising result, a metric must be put to this result so as to quantify the plume model sensitivity to the source.

Sensitivity Analysis

Figures 7 and 8 display the calculated erosion rates for a solar array with a silver surface first using the experimental source and linear-fit sputtering models and then using the experimental source model and the enhanced sputtering model which includes the sputtering yield angular dependence. Figure 7 is the baseline case. The surface is assumed to sit at -92 volts with respect to the center of the plume. These figures suggest that ions striking surfaces at angles which are not normal to the surface significantly affect erosion rates. Using the worst-case scenario, the silver erodes at a rate of 23.1 microns/month at its maximum. This is almost three times as large as the maximum erosion rate in the baseline case and is clearly unacceptable. Interconnectors on solar arrays, which are silver, have an allowable erosion depth of 2.5 microns which translates to an average rate of 1.2 microns/month over the lifetime of the satellite.

However, it should be noted that the surfaces on which the ions strike are being held at a negative potential with respect to the plume. One way to reduce the peak erosion rate is to bias cells at the corners of the array positive with respect to the spacecraft. This would lower the energy of ions striking the surface of the array and help mitigate sputtering losses. Installation of a plume shield might also allay sputtering losses. Modeling the plume in the presence of a plume shield is within the capability of the present simulation but has not yet been completed.

Comparative erosion data for the sensitivity of the different source models are given in Figures 7 and 9. Figure 7 gives the distribution of the erosion of silver

using the experimental source model. The maximum concentration of erosion rate is located at the bottom center of the solar array. Using the hybrid-PIC-derived source model, sputtering becomes more sparse, as seen from Figure 9, and the maximum concentration of the erosion rate is located at the right corner of the array. The erosion rate is also almost twice as large as the sputtering rate using the experimental source model. Although both the source model generated by the hybrid-PIC code and the source model generated from the experimental data may be flawed, they are still applicable in the gauging of the sensitivity of the plume model to various source inputs.

The variation between hybrid-PIC and experimental source model is significant at the exit plane as evidenced by the difference in the erosion rates produced by both source models. The hybrid-PIC model's erosion rate is magnified by as much as twice the rate in some locations, and the model distributes ions much differently than the original data. Thus, the plume model is very sensitive to the input and further tests are needed to fully quantify sensitivity.

Integration Issues

The source model is of utmost importance in the integration of the two models. In addition, code streamlining and optimization, the inclusion of a graphical user interface (GUI), handling the low-frequency discharge oscillatory behavior of the thruster, and the implementation of an unstructured mesh for thruster and satellite geometries must be investigated. The plume model has the ability to simulate the plume structure with both singly- and doubly-ionized Xe propellant emerging from the thruster exit; however, the hybrid-PIC code lacks the formation of Xe double ions. Thus, the hybrid-PIC model must be modified to include the Xe double ions in the ionization process as well as yield an accurate exit plane distribution for ion current density. Total run time on SGI and Dec Alpha workstations is estimated to be 35-40 hours: 20 hours for the hybrid-PIC model and 15-20 hours for the plume model to run.

Conclusions

The 3D plume model developed by Oh has been validated at the microscopic level and has been modified to incorporate the angular dependence of sputtering yield. A

previous value of 34 eV assumed for the axial ion temperature from the thruster proved to be incorrect. The true value is an order of magnitude smaller. The inclusion of sputtering yield angular dependence produces significant differences in erosion rates. Most particles strike the surface at non-normal angles. Sensitivity analysis suggests the 3D plume model is sensitive to the source model as witnessed by erosion data.

Integration of the interior and exterior models would result in a single, stand-alone application describing the thruster physics from the thruster interior through the plume region. The application would enhance the spacecraft design process by providing engineers with the ability to predict thruster performance and damage to the craft from plume-spacecraft interactions given a variety of Hall thruster geometries and characteristics.

Acknowledgments

The authors wish to thank David Manzella at NYMS Inc. for providing data used in this paper and Tom Randolph at SS/Loral for his help constructing a realistic satellite geometry. This paper was funded by the Air Force Office of Scientific Research.

References

- ¹Fife, J.M. "Two-Dimensional Hybrid Particle-in-Cell Modeling of Hall Thrusters." MIT Department of Aeronautics and Astronautics, S.M. Thesis, Cambridge, MA, 1995."
- ²Oh, D.Y. "Computational Modeling of Expanding Plasma Plumes in Space Using a PIC-DSMC Algorithm." MIT Department of Aeronautics and Astronautics, Sc.D. Thesis, Cambridge, MA, February 1997.
- ³Oh, D.Y. and D.E. Hastings. "Axisymmetric PIC-DSMC Simulations of SPT Plumes." IEPC Paper 95-160, September 1995.
- ⁴Fife, J.M. and M. Martinez-Sanchez. "Two-Dimensional Hybrid Particle-in-Cell (PIC) Modeling of Hall Thrusters." IEPC Paper 95-240, September 1995.
- ⁵Fife, J.M., M. Martinez-Sanchez, and J. Szabo. "A Numerical Study of Low-Frequency Discharge Oscillations in Hall Thrusters." AIAA Paper 97-3052, July 1997.
- ⁶Gavryushin, V.M. and V. Kim. "Effect of the Characteristics of a Magnetic Field on the Parameters of an Ion Current at the Output of an Accelerator with Closed Electron Drift." Sov. Phys. Tech. Phys., Vol. 26, No. 4, April 1981, pp. 505-507.

⁷Rosenberg, D. and G.K. Wehner. "Sputtering Yields for Low Energy He⁺-Kr⁺, and Xe⁺-Ion Bombardment." Journal of Applied Physics, Vol. 33, No. 5, May 1962, pp. 1842-1845.

⁸Andersen, H.H. and H.L. Bay. "Sputtering by Particle Bombardment I: Sputtering Yield Measurements." Topics in Applied Physics, Vol. 47, pp. 200-203.

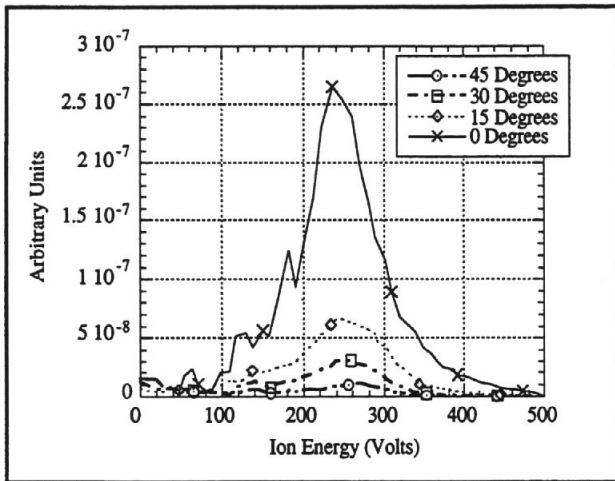


Figure 1. RPA Measurements of Ion Energy Distribution, z = 60 cm

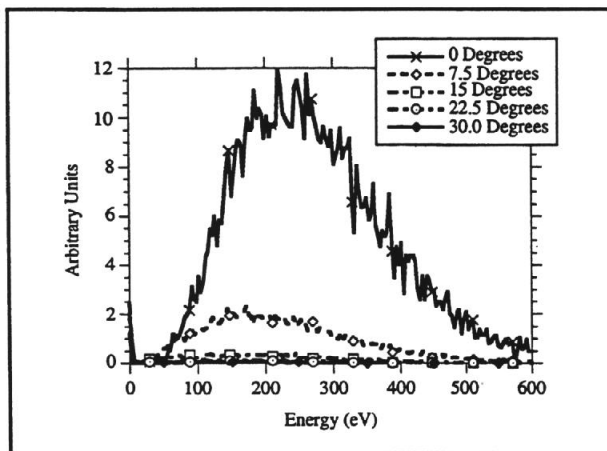


Figure 2. Simulated RPA of Ion Energy Distribution at 34 eV, z = 60 cm

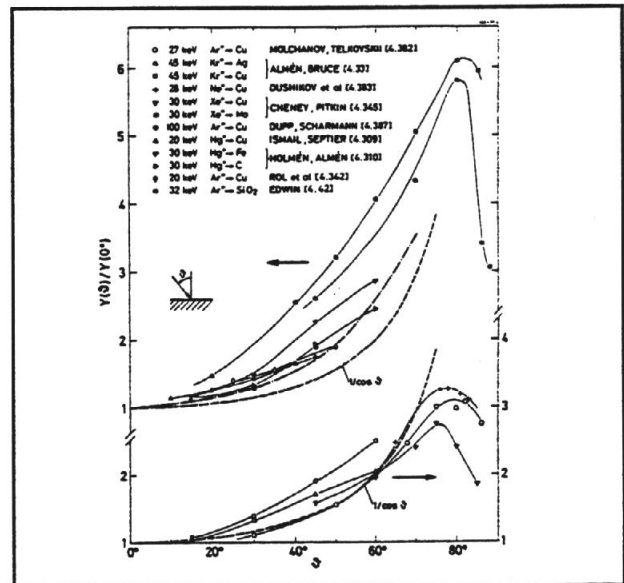


Figure 3. Sputtering yield angular dependence

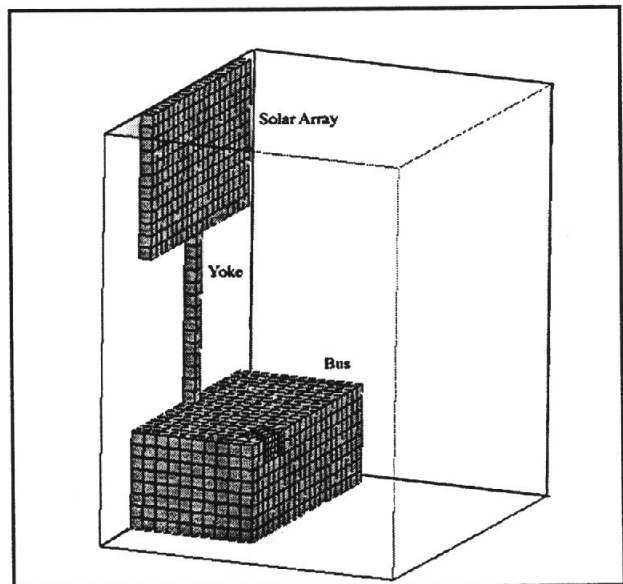


Figure 4. Satellite configuration

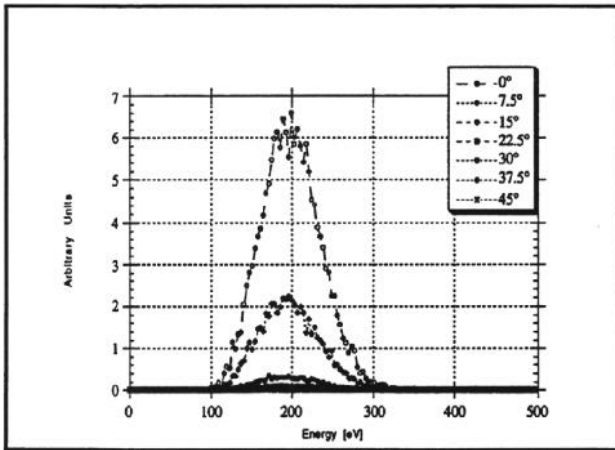


Figure 5. Simulated RPA at 3.4 eV using experimental source model, $z = 60$ cm

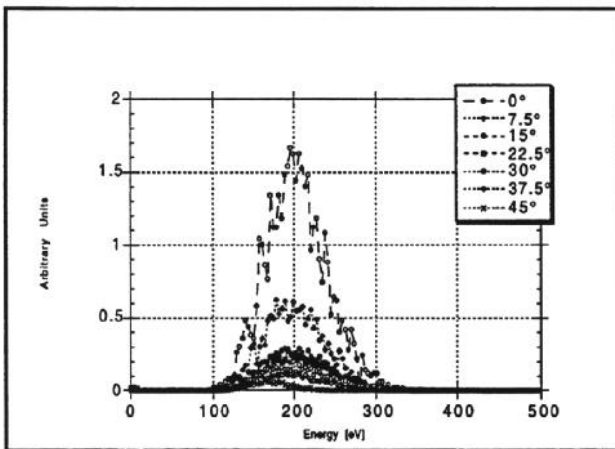


Figure 6. Simulated RPA at 3.4 eV using Hybrid-PIC-derived source model, $z = 60$ cm

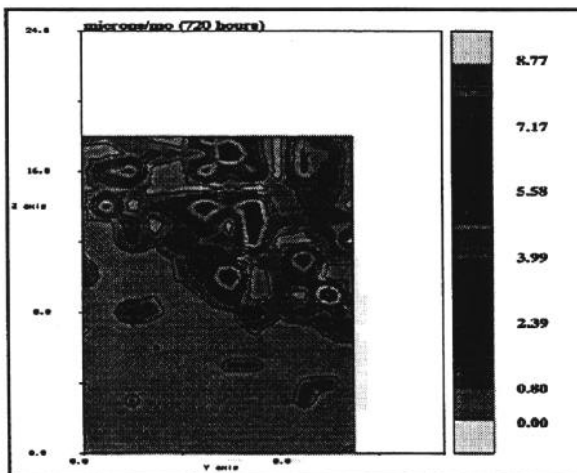


Figure 7. Erosion rate for silver on solar array using original sputtering model and source model

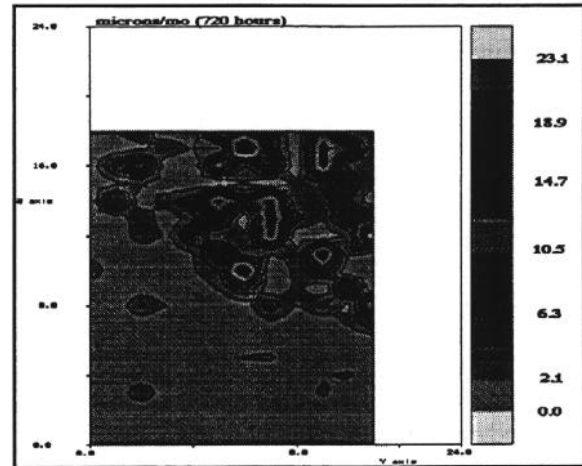


Figure 8. Erosion rate for silver on solar array using modified sputtering model and original source model

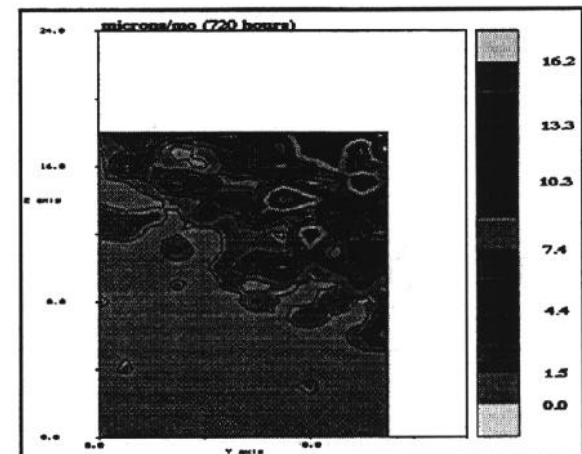


Figure 9. Erosion rate for silver on solar array using modified sputtering and source model